separations

MDPI

Article

Effect of Scale-Up on Residence Time and Uranium Extraction on Annular Centrifugal Contactors (ACCs)

Alastair Baker [1,*], Alex Fells [1], Thomas Shaw [1], Chris J. Maher [2] and Bruce C. Hanson [1]

[1] School of Chemical and Process Engineering, University of Leeds, Leeds LS2 9JT, UK; b.c.hanson@leeds.ac.uk (B.C.H.)
[2] National Nuclear Laboratory, Central Laboratory, Seascale CA20 1PG, UK
* Correspondence: a.r.baker@leeds.ac.uk

Abstract: This work reports the effect of scaling up annular centrifugal contactors (ACCs) upon the residence time distribution and the efficiency of extraction of uranium. The experiments were carried out in a multi-scale ACC platform of three ACCs with rotor diameters of 12, 25, and 40 mm. To enable direct comparison across all three scales of ACC, the residence time distributions were acquired by injecting dye into the solvent phase at a constant relative volume related to the ACC liquid holdup. Across all scales and flowrates, there was little difference in residence time distribution (<6 residence volumes), except for the smallest 12 mm rotor diameter ACC with a high solvent/aqueous feed ratio, which required 12 residence volumes, potentially due to internal circulation in the annulus. At low flowrates, the stage efficiency in all cases was >95%, and it improved further in larger rotor diameter ACCs.

Keywords: annular centrifugal contactor; annular centrifugal extractor; solvent extraction; liquid-liquid extraction; nuclear fuel cycle; residence time distribution; scale-up

check for updates

Citation: Baker, A.; Fells, A.; Shaw, T.; Maher, C.J.; Hanson, B.C. Effect of Scale-Up on Residence Time and Uranium Extraction on Annular Centrifugal Contactors (ACCs). *Separations* **2023**, *10*, 331. https://doi.org/10.3390/separations10060331

Academic Editor: Mohamed F. Attallah

Received: 31 March 2023
Revised: 10 May 2023
Accepted: 23 May 2023
Published: 26 May 2023

1. Introduction

Liquid-liquid extraction is the name chosen by the International Union of Pure and Applied Chemistry (IUPAC) [1]. Liquid-liquid extraction (LLE), which is synonymous with solvent extraction, 'is the process of transferring a dissolved substance from one liquid phase to another (immiscible or partially miscible) liquid phase in contact with it [2]' and shown in Figure 1. The solute 'material can be partitioned into specific fractions which can be extracted selectively by using appropriate reagents' in the process known as Sequential Solvent Extraction [3] or Selective LLE.

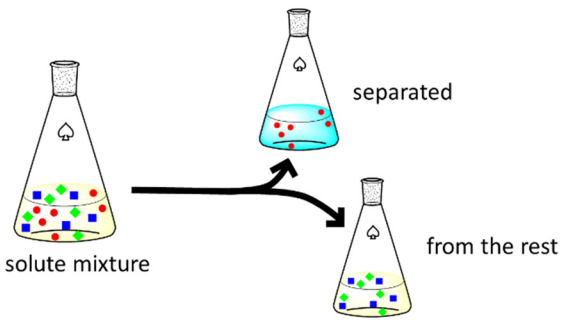

Figure 1. Schematic diagram of Liquid-Liquid Extraction [3].

Liquid-liquid extraction (LLE) has become the preferred method for isolating uranium and plutonium from irradiated fuel in the nuclear fuel cycle (known as reprocessing

within nuclear engineering), surpassing precipitation/recrystallization methods. Batch-wise single-stage extractions performed in chemical laboratories, at a small scale for analytical validation of methods, involve contacting the solution loaded with solute with an immiscible solvent that contains a ligand. The transfer of the solute is driven by a favourable chemical potential for the solute to form a new complex in the solvent containing the ligand.

Traditionally, there are two physical limiting forces for LLE; the mass transfer between the two bulk solutions and the separation of the two solutions by gravity. The intensification of mass transfer is achieved by increasing the surface area of both phases, which is achieved through agitation to produce a dispersion of fine droplets of both phases. However, a dispersion cannot be separated and results in undesirable entrainment, which would require further processing. The driving force for resolving the dispersion, known as coalescing, is a function of the density, also known as volumetric mass density or specific mass, which is a function of the gravitational force applied to the droplets. Currently, the industrial benchmark technologies for LLE are mixer settlers and pulsed columns, both of which rely on gravity and large settling tanks.

Process intensification has been described as 'the development of novel apparatuses and techniques that compared to those commonly used today are expected to bring a dramatic improvement in [. . .] processing substantially decreasing equipment size/production capacity ratio or waste production, and ultimately resulting in cheaper sustainable technologies [4]'.

Process intensification of LLE through increasing the gravitational force reduces the time to resolve the dispersion of two immiscible phases. This results in a reduction in both size and volume of the vessel required [5], known as a settling tank or settling zone. This effect can be achieved through an annular centrifugal contactor (ACC), also known as an annular centrifugal extractor. Alternatively, microfluidic devices are another form of process intensification for LLE that are worthy of note [6], but they are not in the scope of this work. The Advanced Fuel Cycle Programme, which was part of the UK government's Department for Business, Energy, and Industrial Strategy's Energy Innovation Programme, was tasked with the mission of increasing the sustainability of nuclear energy whilst simultaneously minimising the environmental footprint [7]. In the broader context, nuclear energy is part of the solution of removing carbon dioxide from the atmosphere, producing low-carbon emission energy and reaching the legally binding 'net zero' commitments [8]. An aim of the Advanced Fuel Cycle Programme was to develop advanced technologies for recycling spent fuels in the nuclear fuel cycle [8–10].

ACCs are considered as the likely advanced technology for future chemical-separation recycling plants [10,11], as they offer advantages over mixer settlers and pulsed sieve-plate extraction columns [12]. These features make a comparatively more efficient and compact design, figuratively shown in Figure 2.

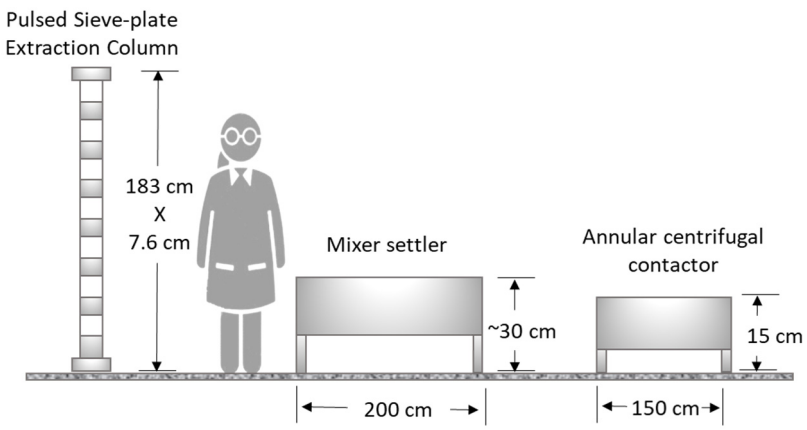

Figure 2. Comparison of annular centrifugal contactors, mixer settlers, and pulsed columns [13].

The main features of an ACC are;

- high shear,
- high-efficiency mixing zone,
- an enhanced separation zone, using centrifugal force that is 200× greater than gravity.

An ACC consists of two cylinders: the outer cylinder is stationary, and the inner hollow cylinder containing static vanes rotates (Figure 3) [5,11,14]. The space between the two cylinders produces an annular mixing region. Typically, two immiscible liquids of different densities are pumped into the annular mixing zone, the void between a stationary outer and an inner rotating cylinder [15,16]. The revolution of the rotor creates a high-shear mixing zone within the annulus and breaks up the two phases into a fine dispersion. The inner cylinder rotation provides sufficient shear to induce Taylor vortexes through turbulent flows and destabilises Couette flow regimes [17]. The internal cylinder rotation simultaneously provides a vertical pumping motion, forcing the fluids downwards, drawing them up into the hollow inner rotating cylinder using guide vanes. The centrifugal force within the inner rotating cylinder then separates the two phases.

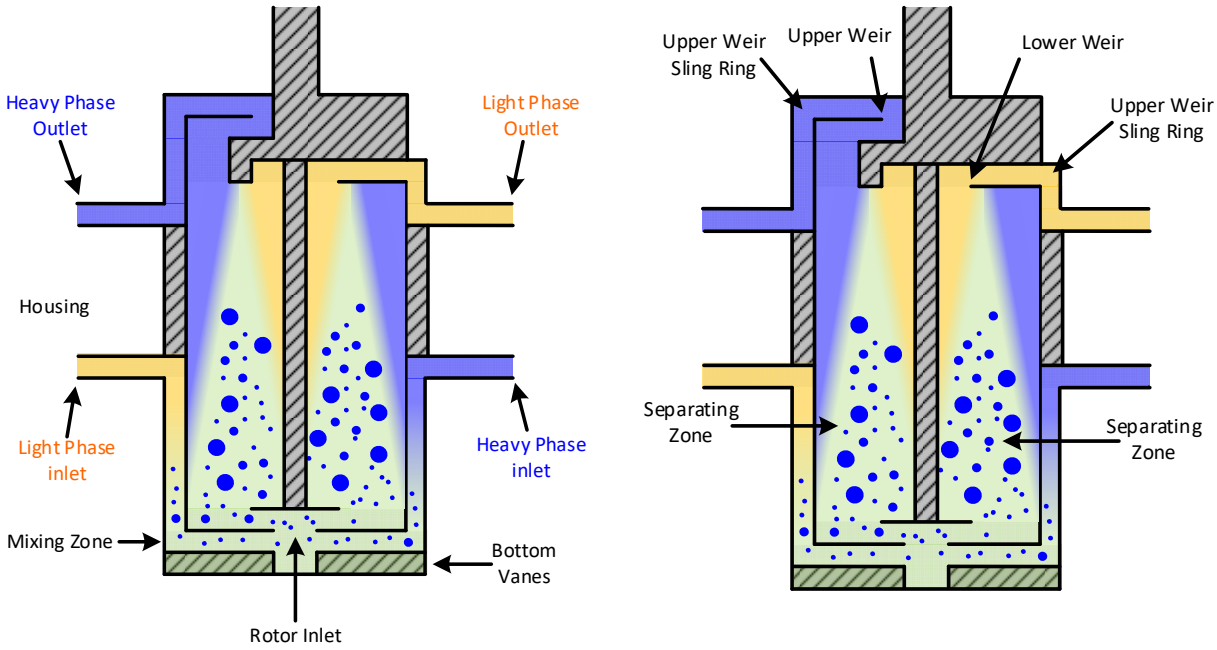

Figure 3. Labelled diagrams of an ACC, (**a**) the housing labelling showing the inlet, annulus mixing zone between the static wall and the rotor, (**b**) the inner hollow rotor in which the mixed dispersion is resolved and the weir in which the phases are separated.

In 1993, the Atomic Energy Authority Technology conducted initial testing of a 55 mm RD Oak Ridge National Laboratory ACC for reprocessing research in the UK [18]. British Nuclear Fuels Limited tested ACCs in the mid-1990s; this led to the development of 1 cm RD Institute of Nuclear and New Energy Technology ACCs and their adoption for flowsheet testing due to their small sizes, which simplifies their use in several active research facilities [19–24]. Flowsheet testing in other research establishments generally uses similarly small ACC cascades [25–29]. Future reprocessing plants may need >20 cm RD ACCs. There are large differences in the scales between laboratory scale flowsheet demonstrations and commercial processes. Knowledge of the effect of scale is necessary to understand process scale-up [14].

There is a body of work in the literature on the hydrodynamics and kinetics of ACCs. However, only one described the experimental evaluation across scales, yet this work

did not specifically look at mass transfer. In a recent review by Vedantam and Joshi in 2006 ACCs, it was stated that 'relatively scanty information is available on the detailed quantitative flow pattern in single and multiphase flows, mixing and axial mixing, mass and heat transfer coefficients, and drop and bubble size distribution [30]'. The gap in how this equipment scales means that any work predating the commissioning of the multi-scale ACC platform will require unification. Additionally, without a complete understanding of the velocity flow fields of an ACC, it is possible to predict the residence time distribution; this requires a suitably validated model and is computationally expensive.

ACCs offer potential significant size advantages over mixer settlers and pulse columns. It is known that ACCs have short residence times that minimise radiation damage to the organic phase [31,32], but they are sensitive to solids, so improved feed conditioning is expected to be necessary. The short resistance times of ACCs minimise contact times between highly radioactive streams that reduce the solvent dose. Understanding ACC behaviour across sizes is important to be able to relate small-scale laboratory flowsheet development studies to pilot scale tests and the larger plant scale. Understanding the relationship between ACC size, flowrate, and stage efficiency will allow for the design of processes with the correct number of ACC stages. Whilst understanding the effect of S/A inside ACCs and resistance distribution time will allow for improvements in ACC and process simulations [7]. The modelling developments will lead to improvements in the following ways. CFD modelling to understand hydrodynamic behaviour and process modelling improvements will allow for a more accurate simulation of the mass transfer and the simulation of chemical reactions that occur inside the ACC on timescales that are similar to the residence times in the ACC [7,33–38].

This work at the University of Leeds examined the effect of scaling up ACCs in terms of their residence time distributions and extraction efficiency. It includes the construction of a multi-scale ACC platform, figuratively shown in Figure 4. This platform was developed under the Advanced Fuel Cycle Programme to support the decision on whether ACCs should be used in any Fourth Generation Nuclear Reprocessing plant by producing data to underpin the scale-up of flowsheet models from lab scale to plant scale [39].

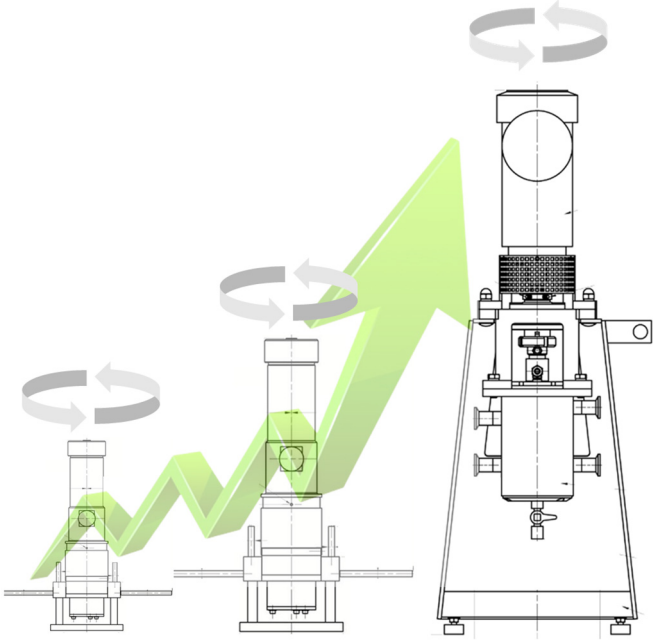

Figure 4. Drawing of lab scale (left, middle) compared to pilot plant scale, with the action of the motors shown perpendicular to gravity.

2. Materials and Methods

2.1. Construction of the Multi-Scale Contactor Rig

A single platform, known as the multi-scale contactor rig (MSCR), was built to use the auxiliary equipment and instruments across multiple scales. The three sizes of ACC were obtained from the BXP series from the commercial supplier Rousselet-Robatel:

- 12 mm RD,
- 25 mm RD,
- 40 mm RD.

The selected ACCs were installed in the Leeds Nuclear Laboratory, and their operating envelope is summarised in Table 1.

Table 1. ACC parameters on the MSCR.

Rotor Diameter	**12**	**25**	**40**	**mm**
Maximum rotor speed	10,000 (670)	4000 (223)	3000 (200)	RPM (G)
Bowl volume	2.2	19	110	mL
Heavy phase weir	7.5	15.5	25.5	mm
Maximum total throughput	33	166	833	mL/min
Minimum total throughput	>3.3	13	83	mL/min
Vanes in mixing zone	4	6	6	-
Height	295	482	792	mm
Width	100	170	312	mm
Weight	5	25	50	kg

Metering pumps were chosen to match the existing United Kingdom National Nuclear Laboratory capabilities [25], and the Q1 1/4" piston diameter pump head (FMI Product QH312N2P0000) was specifically chosen to provide the lowest flowrate of the smallest contactor and the highest flowrate of the largest contactor; from 0.22 to 432 mL/min. However, a key learning from this multi-scale rig would be to use smaller pump heads for lower flows, as recalibrations were required after each run on the smallest ACC. A skeleton drawing of the configuration, Figure 5a, shows the four tanks at the back; one aqueous feed tank with an agitator for suspending solids, one solvent feed tank, and two receiver tanks for the outlet streams. Figure 5b shows the proposed arrangement of the non-active feed tank, pumps, ACCs, and control units.

The bund was constructed from stainless steel. The stand was built from a metal framing system that was 100% reusable, 100% adjustable, and required no welding or drilling, as shown in Figure 5c. The stand was powder coated to prevent corrosion if accidental spillages occurred.

Figure 5d shows the MSCR as built, upon which testing commenced. The as-built iteration included a Perspex panel upon which the ACC rotor control boxes were mounted for accessibility for emergency shutdowns, and the pumps were also placed upon the floor of the bund for accessibility to the pump head while reducing the number of pipe bends, which could result in pressure drops that cause the pumps to stall. The deconstructed 12 mm RD ACC is shown in Figure 6a, and the three sizes of ACC in place are shown in Figure 6b. A complete list of all the components can be found in the Supporting Information.

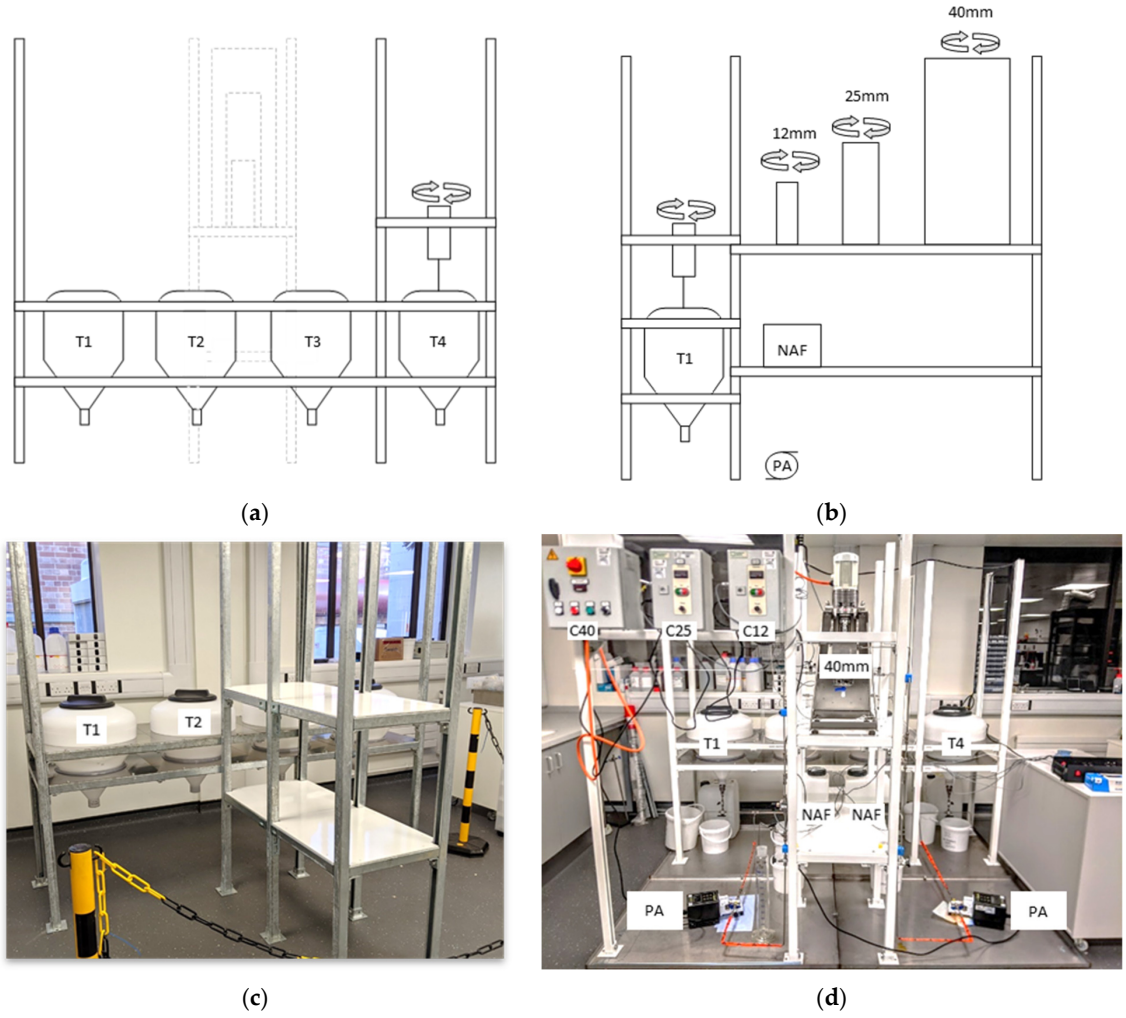

(**a**) (**b**)

(**c**) (**d**)

Figure 5. (**a**) Rear view of the rig housing the tanks (T1–4) in the foreground with the ACC tanks in the background, (**b**) side view showing the agitated aqueous feed tank (T4), the pump (PA) on the floor, the lower shelf housing the non-active feed tank (NAF) and pump, the top-shelf housing the 12 mm, 25 mm, and 40 mm ACCs, (**c**) stand assembled with tanks and horizontal plates in place with tanks T1 and T2 labelled, (**d**) as-built multi-scale centrifugal contactor rig with all electronic components tested, showing the control units for the ACCs (C40, C25, C12), feed tanks (T1 andT4), non-active feed tanks (NAFs), the pumps (PAs) and the 40 mm RD ACC.

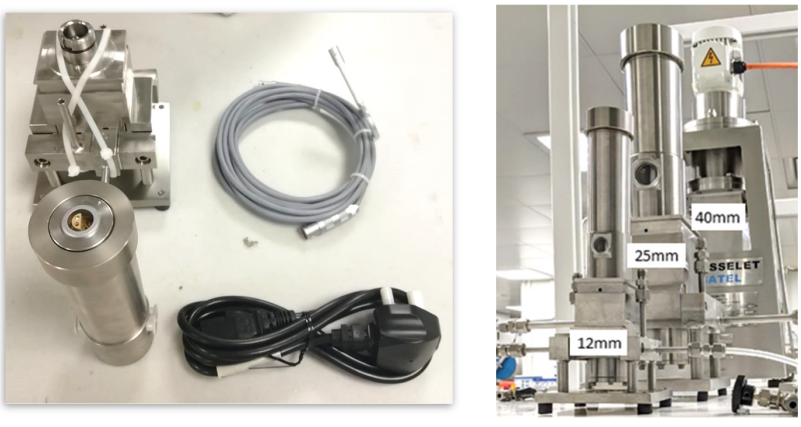

(**a**) (**b**)

Figure 6. (**a**) 12 mm RD ACC components; a housing with rotor installed, motor, power cables, (**b**) from near to far are the ACCs of 12 mm, 25 mm, and 40 mm RD.

2.2. Materials

Uranyl nitrate hexahydrate ($UO_2(NO_3)_2.6H_20$, 98–102%) was procured by ABSCO Ltd., UK, from International Bio-Analytical Industries, Inc., Boca Raton, FL, USA. Nitric acid (>65%, Analytical Reagent, catalogue number 20429.320) and tributyl phosphate (≥99.0%, catalogue number 304886L) were supplied by VWR International. Brenntag supplied Exssol D-80 kerosene (catalogue number EXX0080NF). All materials were used without purification.

2.3. Uranium Solvent Extraction Batch Test

The batch test was performed in a beaker (100 mL), to which the corresponding volumes for a desired S/A were added to an initial aqueous solution of uranium (10 g/L) in nitric acid (1.5 M) in contact with tributyl phosphate (30 vol%) in kerosene (branded Exxsol D-80) with a magnetic stirrer (4 cm). The beaker was placed on a stirrer plate and stirred at 500 RPM for 20 min at room temperature (19 ± 3 °C). The mixture was poured into a separator funnel (50 mL), swilled to force droplets down the sides, and was then allowed to settle for 10 min. The two phases were disengaged, and the samples were placed on a benchtop centrifuge at 6500 rpm for 150 s.

2.4. UV Vis Spectrometer

The Spectrometer Assembly (FLAME-S-UV-VIS, 200–850 nm) with thermoregulator (USB-TC) was connected to a High Power MINI Deuterium Tungsten Halogen Source w/shutter (200–2000 nm) via cuvette holders (either 1 cm path or 10 cm) with 400 um Fiber, solarization-resistant (2 m, P400-2-SR). The system was turned on for 20 min before capturing the first spectrum to ensure the lamp and spectrometer achieved operating temperatures. For the captured spectra, the reference sample was used to collect the background, the 'integration time' was set to 45 ms, and the 'scans to average' was set to 5. Then, the lamp shutter was closed and a dark spectrum was taken.

Two UV-Vis calibrations were produced to allow the quantification of uranium in nitric acid and 30%TBP in D-80 kerosene. The aqueous calibration was prepared by volumetric dilution of a commercial uranium standard (Fishersci 12946434). The solvent calibration was carried out by preparing a series of uranium-loaded TBP in D-80 kerosene samples using different aqueous uranium concentrations. The final aqueous uranium concentration was determined using the aqueous calibration and solvent uranium concentrations calculated.

2.5. Titrations

Titrations were manually performed using a burette (50 ± 0.1 mL) charged with 0.1 M NaOH standard solution. To a beaker (100 mL), a sample of aqueous or solvent (1 mL) was added. Then, deionised water (9 mL) and phenolphthalein (2 vol%, 2–3 drops) in ethanol solution (Honeywell Fluka 74760-100 ML) (3 drops) was added. The sample was titrated with 0.1 M NaOH standard solution. The endpoint was determined upon the sample colour changing from colourless to pink and the volume of titrant was documented. For completeness, the free acidity was also determined by titration of 1 mL samples added to 9 mL of 1 mol/l KF using 0.1 mol/l NaOH. These results were consistent with those expected and are not reported.

2.6. Residence Time Distribution Experiments and Liquid Holdup within ACC Housings

Solvent samples were taken from the solvent phase outlet over designated time steps. The aqueous feed tank was charged with water and the solvent feed tank was charged with D-80 kerosene. The centrifuge motor was started, the aqueous pump was started at its desired flowrate and was allowed to run for 5 min, and then the solvent pump was started and allowed to run for 10 min, at T = 0 s the dye (Sudan Blue II 0.4 g/L in D-80 kerosene) was injected by hand by a single, quick depression of the syringe plunger into the solvent inlet using a tee-piece connected to a syringe. At the end of an experiment, the pumps and

centrifuge were stopped and the liquid holdup within the contactor housing was measured using measuring cylinders (25 ± 0.5 mL and 10 ± 0.2 mL) and syringes (2 ± 0.1 mL).

2.7. Uranium Solvent Extraction with ACCs

The aqueous feed tank was charged with aqueous uranyl nitrate (10 g/L) in nitric acid (1.5 M). The solvent feed tank was charged with reagent grade TBP (30 vol%) in D-80 kerosene. The centrifuge motor was started, at T = 0 min the aqueous pump was started at its desired flowrate, at T = 5 min the solvent pump was started; at T = 25 min, liquid samples were taken from the aqueous phase outlet and solvent phase outlet over designated time steps. The samples were volumetrically measured using measuring cylinders (100 ± 0.5 mL and 10 ± 0.1 mL). At the end of the experiment, non-active feed containing no uranium was pumped through the ACCs at high flowrates to decontaminate the ACCs.

2.8. Working with Open Sources of Ionising Radiation

All work with radioactive substances at the University of Leeds is carried out under a strict management protocol to ensure compliance with health, safety, and environmental legislation. Ionizing radiation is radiation that has the power to charge (ionize) atoms. In the human body, this ionization can cause adverse health effects such as the induction of cancer. The risk of an adverse health effect is related to the level of exposure to radiation, and the risks are, therefore, controlled by limiting the exposure of workers to radiation. Radiation workers have to complete radiation safety training, log risk assessments, order and confirm the receipt of sources, record the usage of sources, and log radioactive waste disposal.

Only individuals holding a valid University of Leeds Radiation Work Permit are permitted to handle unsealed radioactive substances. The University's permits for radiation work, issued under the Environmental Permitting Regulations 2010, specify that 'Best Available Techniques' must be used to minimize the radiological impact of discharges on people and the environment. Contamination control techniques are used to minimize the creation and spread of contamination, as follows:

- Careful dispensing and handling of any material to minimize the risk of contamination.
- Immediate disposal of any contaminated tips, syringes, etc.
- Containment of any samples created in a secondary container such as a plastic bag or box.
- Storage or disposal of any stocks and samples not in use as soon as practicable.
- A radiation monitor is used to identify any contaminated areas or equipment.

3. Results and Discussion

Volumetric holdup is a term used in chemical engineering to describe the amount of liquid within a reactor; in this manuscript, it is the amount of liquid within an ACC. It represents the actual liquid volume rather than using the static free space available in an ACC. It is an important parameter in the design and optimization of chemical processes that involve the flow of liquids, as it affects the efficiency of mass transfer and reaction kinetics.

During the operation of an ACC, the volumetric holdup varies due to several factors; the void volume in the bowl [40], the ratio of solvent, total throughput, and the solvent/aqueous (S/A) ratio. As ACCs operate with high shear mixing and centrifugal force, the liquid holdup is reduced relative to the void volume. The equipment may also suffer from stagnant regions within the vessel, internal recirculation, or a channelling of the fluid. Ideally, understanding these flow types would improve the mass transfer performance and stage efficiency modelling. For a given system, different molecules that enter a vessel will have a range of residence times, with some molecules exiting almost immediately, while others remain in the system much longer. The distribution of these times is known as the fluid's residence time distribution (RTD) and is measured in s^{-1}.

In this work, there were three specific techniques to determine two of the factors affecting the performance of ACCs:

1. Residence time
2. Volumetric holdup
3. Residence time distribution
4. Extraction stage efficiency of uranium (in the species of uranyl nitrate item)

An experimental matrix, as shown in Table 2, was developed to encompass an extreme operational range of S/A ratios. Of the flowsheets (of use to ACCs) that have developed so far [11], these extreme S/A ratios would likely be the upper limits of a future recycling plant. In all cases, to evaluate the conditions with the greatest residence time, the minimum total throughput (also known as the combined flowrate of both phases), as stated by the supplier, was used in these studies. Entries 2, 4, and 7 had multiple runs performed for method development and the validation of results. Plotting the RTD on a phase volume basis required the measurement of the solvent phase holdup to enable the comparison of multiple RTDs across scales. The solvent and aqueous holdups were measured at the end of the experiment when the separation rotor and flows simultaneously shut off. These values are reported in Table 2 and plotted in Figure 7. Comparing the solvent (Figure 7a) and aqueous (Figure 7b) holdup clearly shows that the solvent holdup is lower than the aqueous holdup, showing a positive correlation with rotor diameter. The log-log plots, displayed in Figure 7c,d, show a linear trend, implying a power-law relationship between the two variables. This is expected as the vessels' equipment are cylinders of the volume derived from the diameter squared.

Table 2. Experimental matrix for RTDs measured solvent and aqueous holdup.

Entry	Rotor Diameter (mm)	Total Throughput (mL/min)	Rotor Speed (RPM)	S/A Ratio	Number of Repeats	Solvent Holdup (mL)	Aqueous Holdup (mL)
1	12	3.3	9500	1:1	3	1.0	1.0
2	12	3.3		1:5.6	1	1.0	1.0
3	12	3.3		6.7:1	1	1.0	1.0
4	25	13.0	3500	1:1	3	4.5	17.0
5	25	13.0		1:5.6	1	6.5	14.5
6	25	13.0		6.7:1	1	8.5	16.0
7	40	83.0	2500	1:1	3	50.0	89.0
8	40	83.0		1:5.6	1	29.0	104.0
9	40	83.0		6.7:1	1	54.0	80.0

RTDs were experimentally determined by injecting a dye into the solvent inlet of an ACC and regularly sampling the outlet to determine the concentration. In this study, Sudan Blue II, Figure 8a, dissolved in the solvent phase, was selected due to its UV-Vis compatibility. The injection point on the 25 mm RD ACC is shown in Figure 8b. For this investigation, dye injection volumes, equating to approximately 4% of the experimentally derived liquid holdup in each ACC and listed in Table 3, were used to keep any disruption to the hydrodynamics to a minimum and maintain a steady state.

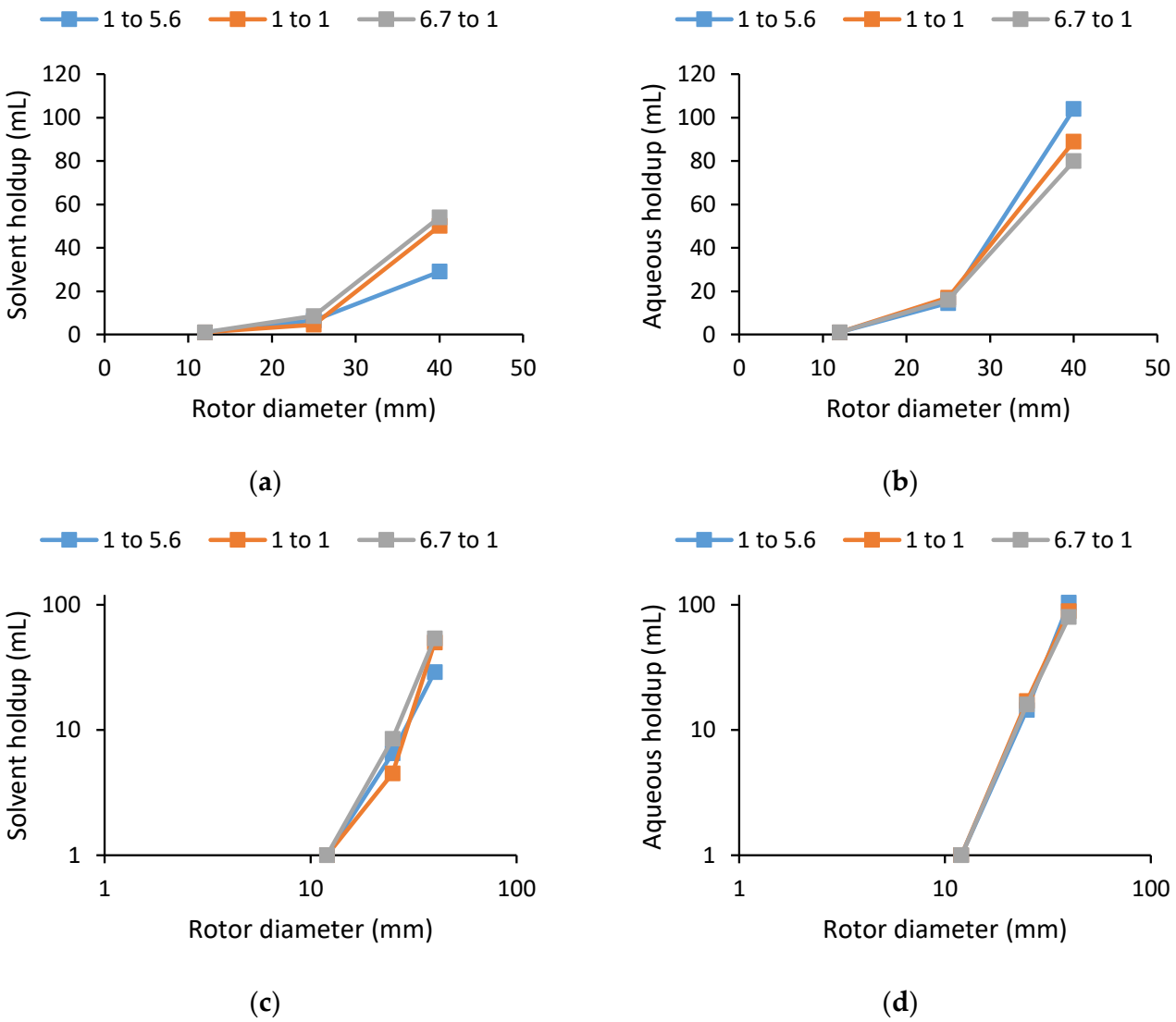

Figure 7. Phase holdup against rotor diameter for: (**a**) solvent phase; (**b**) aqueous phase; (**c**) solvent phase on a log-log basis; (**d**) aqueous phase on a log-log basis.

Figure 8. (**a**) Structure of Sudan Blue II, (**b**) injection pipework.

Table 3. Dye injection volumes relative to ACC volumes to enable comparisons.

Rotor Diameter (mm)	Experimentally Derived Liquid Holdup (mL)	4% by Volume Dye Injection (mL)
12	2.7	0.1
25	25.3	1.0
40	143.0	5.5

To enable the comparison of multiple RTD curves, the data was normalised so that the area was equal to 1.

$$\int_0^\infty RTDdt = 1$$

As a result of measuring the liquid holdup values, the actual residence volumes were estimated using the following equation:

$$Residence\ volume = \frac{time \times phase\ flowrate}{phase\ holdup}$$

Figure 9a–c shows the normalised RTDs expressed on a time basis for all three contactors for S/A ratios 1 to 5.6, 1 to 1, and 1 to 6.7, increasing in rotor diameter size from right to left. The RTD curves across all S/A ratios exhibit positive skew and an approximately log-normal distribution. A comparison of Figure 9a with the smallest 12 mm RD ACC shows that the residence time and RTD appear to increase with decreasing S/A ratio; however, this trend is not observed in the larger 25 or 40 mm RD ACC. By expressing RTD on a solvent volume basis, the contrast is more definitive in that larger contactors are less susceptible to recirculation of the solvent phase and likely have different internal hydrodynamics [40]. The flattening of the RTD peaks for the 40 mm RD ACC is likely caused by insufficient sampling frequency curtailing the peak.

For the 12 mm RD ACC, as the S/A ratio increases, the residence times (Figure 10d) and solvent residence volumes (Figure 10) are reduced. This could indicate that the solvent is being recirculated within the contactor with low solvent flowrates compared to the aqueous flowrates. A comparison of plots Figure 10d–f indicates relatively little difference on a solvent residence volume basis, with most of the tracer flushed through within six residence volumes, except for the 1 to 5.6 S/A ratio run performed on the 12 mm RD ACC ACC, which requires 12 residence volumes. This suggests significant solvent recirculation, likely caused by the low solvent flowrate. It has been reported that to determine the physical scale-up characteristics of the ACCs, the aspect ratio is a better quantification and those results showed that a 12 mm RD ACC does not have the equivalent aspect ratio properties and, therefore, cannot be assumed to have comparative physical dimensions to other ACCs and cannot be scaled up.

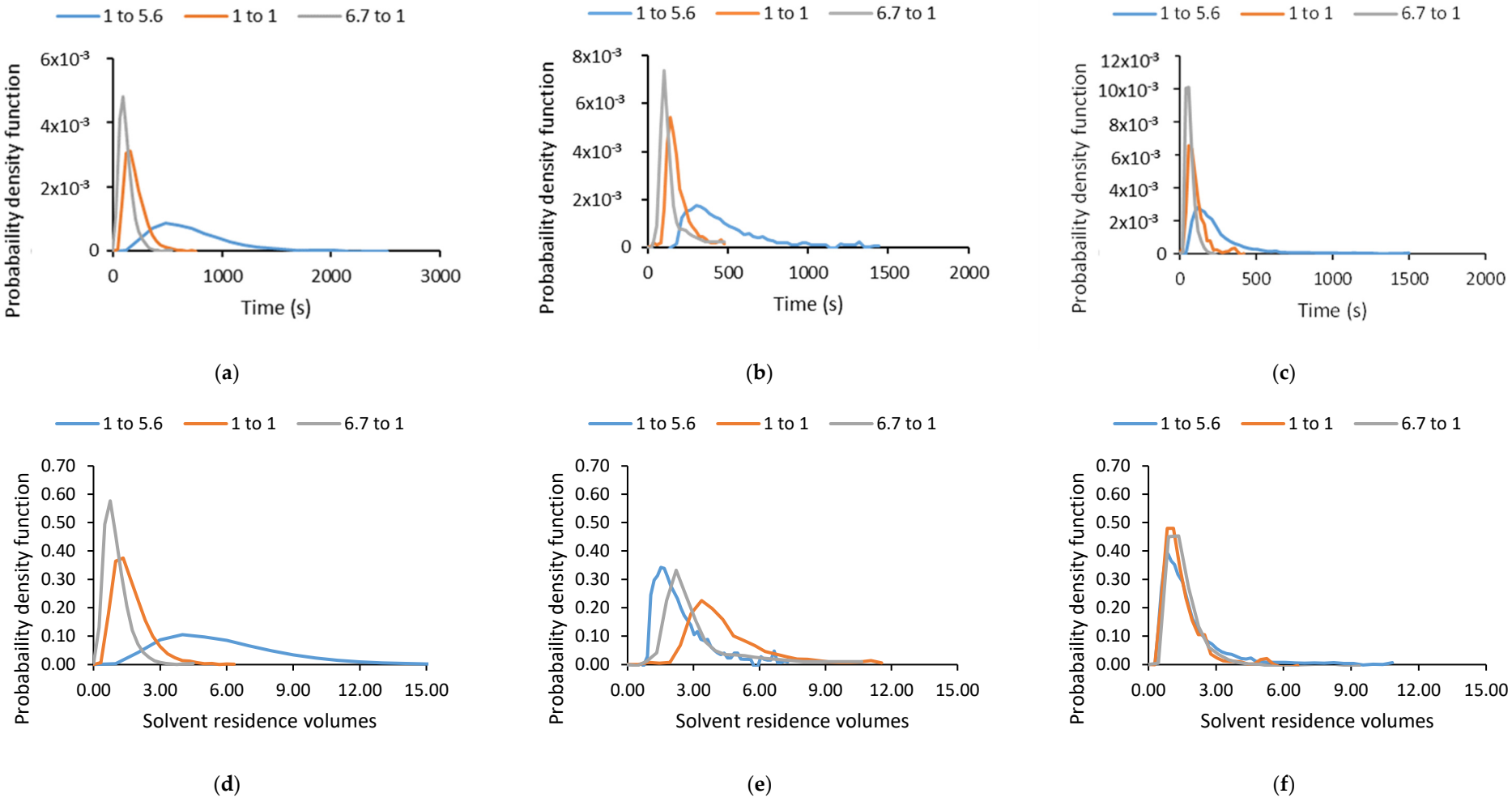

Figure 9. Normalised RTD curves expressed on a time basis for: (**a**) 12 mm RD; (**b**) 25 mm RD; (**c**) 40 mm RD. Normalised RTD curves expressed on a solvent residence volume basis for: (**d**) 12 mm RD; (**e**) 25 mm RD; (**f**) 40 mm RD.

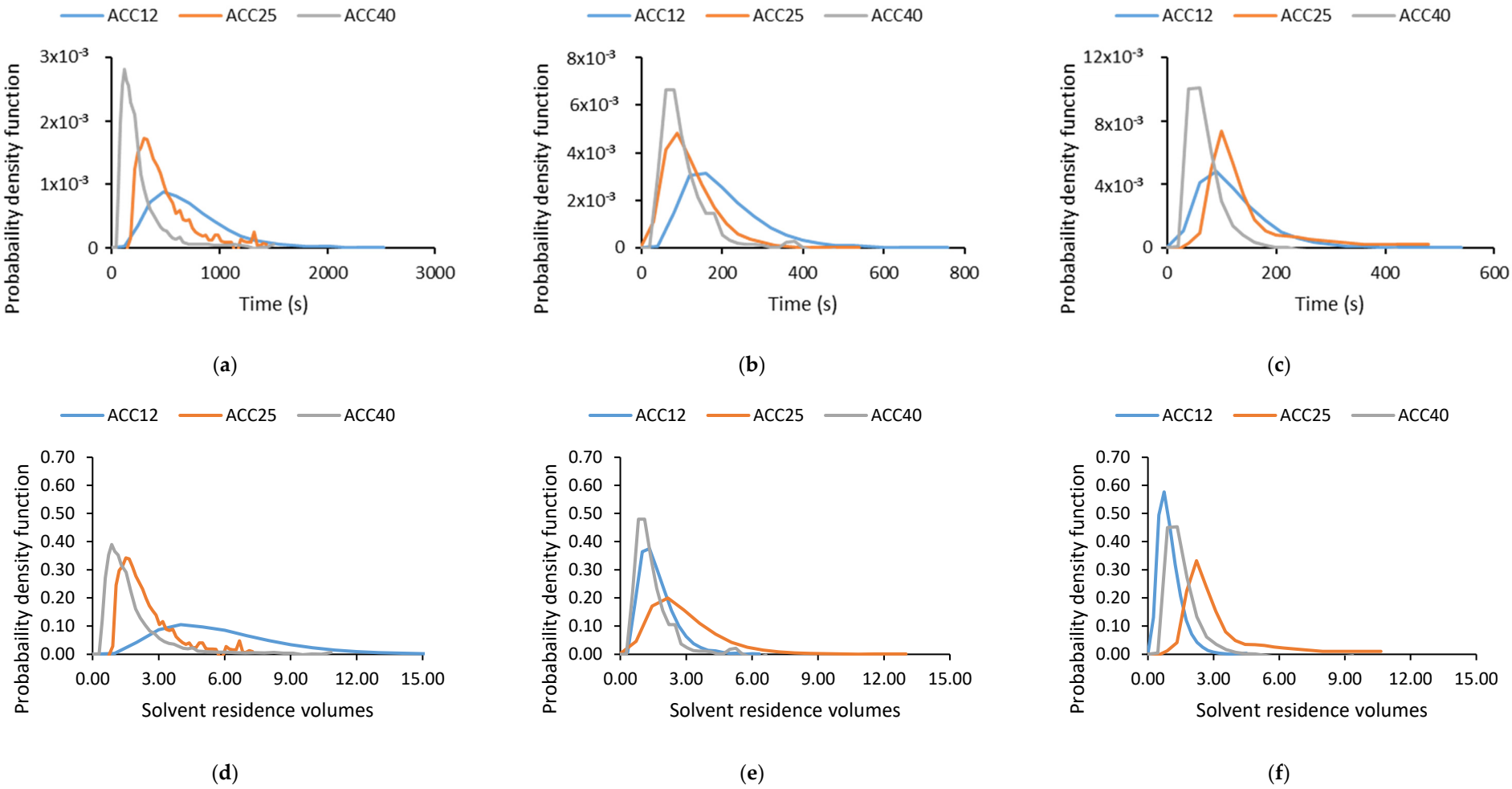

Figure 10. Normalised RTD curves expressed on a time basis for: (**a**) S/A ratio 1 to 5.6; (**b**) S/A ratio 1 to 1; (**c**) S/A ratio 6.7 to 1. Normalised RTD curves expressed on a solvent residence volume basis for: (**d**) S/A ratio 1 to 5.6; (**e**) S/A ratio 1 to 1; (**f**) S/A ratio 6.7 to 1.

Measurement of Stage Efficiency of Uranium Extractions

The investigated chemical system was a simulant of the Plutonium Uranium Reduction [40] Extraction (PUREX) process. This process utilizes the organic extractant tributyl phosphate (TBP) to extract plutonium and uranium ions from an acidic aqueous solution. The TBP forms a complex with the metal ions, which is then extracted into the organic solvent phase shown in Scheme 1, typically kerosene, as it is readily available, cost-effective, and has a low vapor pressure. In our study, an aqueous solution of uranium in nitric acid was contacted with a solvent phase consisting of 30% vol. TBP and Exxsol D 80 kerosene.

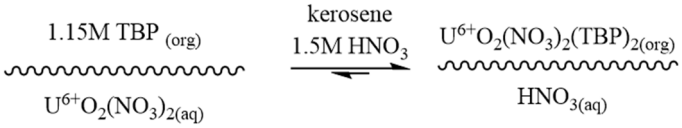

Scheme 1. Chemical equation of the uranium extractions, the oscillating line indicates the solvent/aqueous interface between the two phases.

The second phase of this work was to examine the effect of high and low S/A ratios upon the extraction of uranium using stage efficiency (S.E.). S.E. in a single ACC is calculated by comparison of the initial and final concentrations with the final aqueous at equilibrium, so S.E. = 1.00 is equivalent to the equilibrium.

$$S.E. = ([U]_{initial\ aqueous} - [U]_{final\ aqueous})/([U_{initial\ aqueous}] - [U]_{equilibrium})$$

To assess the quality of the data, mass balances (M.B.) are calculated as a measurement of the accuracy of the data. M.B. is expressed as a ratio of the initial and final uranium concentrations. A mass balance greater or less than 100% indicates a bias in an analytical method or an experimental variable, such as flowrate.

$$M.B.\ (\%) = 100([U]_{initial\ aqueous}\ X\ Aqeuous.Volume)/(([U]_{final\ aqueous}\ X\ Aqeuous.Volume) + ([U]_{final\ solvent}\ X\ Solvent.Volume))$$

The experiments took account of the proposed extremes that may be used in future UK advanced plutonium uranium reduction extraction (PUREX) flowsheets, namely a high S/A ratio of 6.7:1 and a low S/A ratio of 1:5.6. In the experiments performed, the minimum feed flowrates prescribed by the manufacturer were used.

The detection limit (0.2 g/L uranium) of the UV/vis spectroscopy was used. However, using the initial aqueous concentration of uranium (10 g/L) after contact with the large volumes of solvent used with a high S/A ratio, 6.7:1, resulted in a final aqueous uranium concentration that was below this limit of detection and prevented the calculation of accurate stage efficiency and mass balance, which meant the proposed high S/A ratio had to be revised and reduced.

As the experimental campaign progressed and experiments were performed for longer durations than the RTD experiments, it became clear that there was a deviation of the total flowrate to the ACCs, creating an error in the mass balance calculations. Therefore, a series of batch tests were used to determine the highest S/A ratio that could enable measurement using UV/vis spectroscopy and calculate a mass balance. The S/A ratio of the 2:1 batch test produced a final aqueous sample containing 0.214 g/L of uranium, and thus a 2:1 S/A ratio was used in the revised experimental matrix. During the operation of each experiment, the volumes from the outlets of both phases were collected and used to calibrate the actual flowrate, with a corresponding change in the actual S/A ratios required, as shown in Table 4.

Table 4. Actual experimental matrix based upon volumetric measurements of the outlets of both phases.

Entry	Rotor Diameter (mm)	S/A Ratio	Measured Total Throughput (mL/min)	Rotor Speed (RPM)
1	12	2.1:1	1.5	9500
2	25	2.0:1	14.5	
3	40	2.4:1	80.5	3500
4	12	1:7.1	3.5	
5	25	1:6.4	13.8	2500
6	40	1:5.8	81.7	

To determine the effect of the size and scale of ACCs on stage efficiency (SE), the uranium was extracted from an aqueous solution of uranium (10 g/L) in nitric acid (1.5 M) in contact with TBP (30 vol%), diluted in kerosene (branded Exxsol D-80, the supporting information contains the hydrocarbon chain composition). For each entry in Table 3, the rotor motor was started first, followed by the aqueous phase feed, followed by the solvent feed, and allowed to reach stable outlet feeds.

The results of the high S/A ratio showed that, for the 12 mm RD ACC (Table 5), 25 mm RD ACC (Table 6), and 40 mm RD ACC (Table 7), the SE was >96% for all three sizes of ACC with a mass balance of ±10% and the time taken to reach the steady state as a function of increasing rotor size.

Table 5. Results of aqueous uranium solvent extraction in the 12 mm RD ACC with a rotor speed of 9500RPM, the S/A ratio was 2.1 to 1 with a total throughput of 1.5 mL/min.

	Time (min)				
	25	**45**	**65**	**85**	**105**
S.E.	93%	97%	96%	97%	96%
M.B.	84%	89%	90%	90%	89%

Table 6. Results of aqueous uranium solvent extraction in the 25 mm RD ACC with a rotor speed of 3500RPM, the S/A ratio was 2.0 to 1 with a total throughput of 14.5 mL/min.

	Time (min)				
	20	**25**	**30**	**35**	**40**
S.E.	97%	98%	99%	99%	99%
M.B.	104%	95%	97%	94%	96%

Table 7. Results of aqueous uranium solvent extraction in the 40 mm RD ACC with a rotor speed of 2500RPM, the S/A ratio was 2.4 to 1 with a total throughput of 80.5 mL/min.

	Time (min)			
	25	**27**	**29**	**33**
S.E.	97%	98%	98%	98%
M.B.	113%	109%	110%	110%

The result of low S/A ratios for the 12 mm RD ACC (Table 8), 25 mm RD ACC (Table 9), and 40 mm RD ACC (Table 10) showed that the S.E. was >96% for all three sizes of ACC with a mass balance of ±10%. However, the 25 mm RD ACC did present an

issue of reaching a steady state with such low solvent flowrates under the experimental conditions tested.

Table 8. Results of aqueous uranium solvent extraction in the 12 mm RD ACC with a rotor speed of 9500RPM, the S/A ratio was 1 to 7.1 with a total throughput of 3.5 mL/min.

	Time (min)				
	20	**25**	**30**	**35**	**40**
S.E.	93%	97%	96%	97%	96%
M.B.	90%	94%	93%	94%	93%

Table 9. Results of aqueous uranium solvent extraction in the 25 mm RD ACC with a rotor speed of 3500RPM, the S/A ratio was 1:6.4 with a total throughput of 13.8 mL/min.

	Time (min)				
	40	**50**	**55**	**60**	**40**
S.E.	90%	87%	91%	96%	90%
M.B.	92%	91%	90%	107%	92%

Table 10. Results of aqueous uranium solvent extraction in the 40 mm RD ACC with a rotor speed of 2500RPM, the S/A ratio was 1 to 5.8 with a total throughput of 81.7 mL/min.

	Time (min)					
	25	**27.5**	**30**	**32.5**	**35**	**38.5**
S.E.	97%	97%	99%	98%	99%	99%
M.B.	112%	108%	111%	109%	110%	107%

4. Conclusions

ACCs have a wide range of operations. This work aims to increase understanding of the operating envelope of the BXP series of ACCs; specifically, their holdup, residence times, and stage efficiencies for uranium across the extremes of the S/A ratio. With respect to the first area of investigation, the liquid holdup did not significantly vary as a function of total throughput under the conditions studied; however, within an ACC during operation, the S/A ratio was lower than the feed ratio.

ACC residence time was investigated using solvent dye injection and appeared independent of S/A ratios tested for the 25 mm RD ACC and 40 mm RD ACC ACCs, with a maximum residence time equivalent to 6 volumes and a mean residence time of approximately 1.5–2 volumes. The 12 mm RD ACC at a low S/A ratio (1 to 5.6) showed a definite difference with a maximum residence time of 12 volumes, and is a scale-up concern that requires further investigation in future work. Future work could investigate the effect of using ultra-low flowrates to take advantage of the solvent liquid holdup discovered due to the RTD dye injections and using aqueous dyes to follow the aqueous liquid holdup.

The stage efficiencies studied showed little variation in either size or S/A ratio, with >96% stage efficiencies recorded. The total throughput was at the low end of the manufacturer's recommended value. Further work to investigate the effect of total throughput and S/A on stage efficiency will improve knowledge of scale-up.

Author Contributions: Conceptualization, A.B., B.C.H. and C.J.M.; methodology, A.B., B.C.H. and C.J.M.; validation, A.B., A.F. and C.J.M.; formal analysis, A.B. and A.F.; investigation, A.B., B.C.H., A.F. and T.S.; data curation, A.B. and A.F.; writing—original draft preparation, A.B.; writing—review and editing, A.B., A.F., T.S., B.C.H. and C.J.M.; visualization, A.B. and A.F.; supervision, B.C.H. and C.J.M.; project administration, B.C.H. and C.J.M.; funding acquisition, B.C.H. All authors have read and agreed to the published version of the manuscript.

Funding: This research was funded under "the £46M Advanced Fuel Cycle Programme as part of the Department for Business, Energy and Industrial Strategy's (BEIS) £505m Energy Innovation Programme", and by "Engineering and Physical Sciences Research Council (EPSRC) Grant number: 2109068", and by "Engineering and Physical Sciences Research Council (EPSRC) Grant number: EP/S022295/1".

Acknowledgments: We would like to thank Christopher A. Bulman for technical support in the operation of Leeds Nuclear Lab, and the Nuclear Engineering Group at UoLeeds for stimulating discussion and peer review.

Conflicts of Interest: The authors declare no conflict of interest.

Acronyms

ACC	Annular Centrifugal Contactors
RTD	Residence Time Distribution
RD	Rotor Diameter
IUPAC	International Union of Pure and Applied Chemistry
LLE	Liquid-Liquid Extraction
PUREX	Plutonium Uranium Reduction Extraction
MSCR	Multi-Scale Contactor Rig
TBP	Tributyl Phosphate
S/A	Solvent/Aqueous Ratio
RPM	Revolutions per minute
SE	Stage Efficiency
EPSRC	Engineering and Physical Sciences Research Council
BEIS	Department for Business, Energy and Industrial Strategy's

References

1. Leigh, G.J. *Principles of Chemical Nomenclature: A Guide to IUPAC Recommendations*; Royal Society of Chemistry: London, UK, 2011.
2. Rice, N.M.; Irving, H.M.N.H.; Leonard, M.A. Nomenclature for liquid-liquid distribution (solvent extraction) (IUPAC Recommendations 1993). *Pure Appl. Chem.* **1993**, *65*, 2373–2396. [CrossRef]
3. Tessier, A.; Campbell, P.G.; Bisson, M. Sequential extraction procedure for the speciation of particulate trace metals. *Anal. Chem.* **1979**, *51*, 844–851. [CrossRef]
4. Stankiewicz, A.I.; Moulijn, J.A. Process intensification: Transforming chemical engineering. *Chem. Eng. Prog.* **2000**, *96*, 22–34.
5. Hamamah, Z.A.; Grützner, T. Liquid-Liquid Centrifugal Extractors: Types and Recent Applications—A Review. *ChemBioEng Rev.* **2022**, *9*, 286–318. [CrossRef]
6. Xu, C.; Xie, T. Review of microfluidic liquid–liquid extractors. *Ind. Eng. Chem. Res.* **2017**, *56*, 7593–7622. [CrossRef]
7. Baker, A.; De Santis, A.; Fells, A.; Hunter, T.; Hanson, B.C.; Maher, C.; Taylor, R. The development of centrifugal contactors: Next generation solvent extraction equipment for advanced reprocessing of nuclear fuels. *Nucl. Future* **2022**, *3*, 38–54.
8. Barron, N. A 'fast' approach to net zero. *Nucl. Future* **2021**, *17*, 39–45.
9. Goddard, D.T. Recent progress in accident tolerant fuels. *Nucl. Future* **2017**, *13*, 40–44.
10. Nevitt, P.; Sherock, M.; Vernon, E. Fuelling Net Zero—The UK Advanced Fuel Cycle Programme (AFCP). *Nucl. Future* **2021**, *17*, 45–54.
11. Baker, A.; Fells, A.; Carrott, M.J.; Maher, C.J.; Hanson, B.C. Process intensification of element extraction using centrifugal contactors in the nuclear fuel cycle. *Chem. Soc. Rev.* **2022**, *51*, 3964–3999. [CrossRef]
12. Taylor, R. *The Chemical Basis for Separating Recycling Materials by Hydro-Processes*; Elsevier: Amsterdam, The Netherlands, 2021.
13. Law, J.; David, M.; Troy, G.; Nick, M.; Scott, H. The testing of commercially available engineering and plant scale annular centrifugal contactors for the processing of spent nuclear fuel. In Proceedings of the 15th Pacific Basin Nuclear Conference, Sydney, Australia, 15–20 October 2006; Australian Nuclear Association: Sydney, Australia, 2006.
14. Vedantam, S.; Joshi, J. Annular centrifugal contactors—A review. *Chem. Eng. Res. Des.* **2006**, *84*, 522–542. [CrossRef]
15. Webster, D.; Jennings, A.S.; Kishbaugh, A.A.; Bethmann, H.K. Performance of Centrifugal Mixer-Settler in the Reprocessing of Nuclear Fuel. In *Symposium on Recent Advances in Reprocessing of Irradiated Fuel American Institute of Chemical Engineers Meeting*; Du Pont de Nemours (EI) and Co., Aiken, SC Savannah River Lab: New York, NY, USA, 1967.
16. Bernstein, G.J.; Grosvenor, D.E.; Lenc, J.F.; Levitz, N.M. *Development and Performance of a High-Speed, Long-Rotor Centrifugal Contactor for Application to Reprocessing LMFBR Fuels*; ANL-7968; Argonne National Laboratory: Lemont, IL, USA, 1973; p. 52.
17. Miller, J.M.J. *Solvent Extraction and Mass Transfer Assessment in Novel Extraction Technologies*; University of Leeds: Leeds, UK, 2021.
18. Jenkins, J.A.; Thompson, P.J.; Jubin, R.T. Performance of centrifugal contactors on uranium and plutonium active PUREX flowsheets. In Proceedings of the International Solvent Extraction Conference, York, UK, 9–15 September 1993.
19. Birkett, J.; Carrot, M.J.; Fox, O.D.; Maker, C.J.; Route, C.V. *Plutonium and Neptunium Stripping in Single Cycle Solvent Extraction Flowsheets: Recent Progress in Flowsheet Testing*; Nuclear Sciences and Technology Services: Sellafield, UK, 2004.

20. Birkett, J.; Carrott, M.J.; Crooks, G.; Fox, O.D. Purex Process Improvements for PU and NP Control in Total Actinide Recycle Flowsheets. In Proceedings of the Waste Management Symposium, Tucson, AR, USA, 23–25 October 2006; pp. 1–11.
21. Carrott, M.J.; Fox, O.D.; Maher, C.J.; Mason, C.; Taylor, R.J.; Sinkov, S.I.; Choppin, G.R. Solvent extraction behavior of plutonium (IV) ions in the presence of simple hydroxamic acids. *Solvent Extr. Ion Exch.* **2007**, *25*, 723–745. [CrossRef]
22. Fox, O.; Carrott, M.J.; Gaubert, E.; Woodhead, D.A. Development and validation of process models for minor actinide separations processes using centrifugal contactors. In Proceedings of the 7th International Conference on Advanced Nuclear Fuel Cycles and Systems (GLOBAL 2007), Boise, ID, USA, 9–13 September 2007.
23. Carrott, M.; Geist, A.; Hères, X.; Lange, S.; Malmbeck, R.; Miguirditchian, M.; Modolo, G.; Wilden, A.; Taylor, R. Distribution of plutonium, americium and interfering fission products between nitric acid and a mixed organic phase of TODGA and DMDOHEMA in kerosene, and implications for the design of the "EURO-GANEX" process. *Hydrometallurgy* **2015**, *152*, 139–148. [CrossRef]
24. May, I.; Birkett, E.J.; Denniss, I.S.; Gaubert, E.T.; Jobson, M. Mass Transfer Trials on U (VI) and Np (IV) in a Single Stage Centrifugal Contactor. In *Atalante 2000*; CEA Marcoule: Chusclan, France, 2000.
25. Carrott, M.J.; Maher, C.J.; Mason, C.; Sarsfield, M.J.; Whittaker, D.; Taylor, R.J. Experimental Test of a Process Upset in the EURO-GANEX Process and Spectroscopic Study of the Product. *Solvent Extr. Ion Exch.* **2022**, *41*, 88–117. [CrossRef]
26. Wilden, A.; Modolo, G.; Schreinemachers, C.; Sadowski, F.; Lange, S.; Sypula, M.; Magnusson, D.; Geist, A.; Lewis, F.W.; Harwood, L.M.; et al. Direct selective extraction of actinides (III) from PUREX raffinate using a mixture of CyMe4BTBP and TODGA as 1-cycle SANEX solvent part III: Demonstration of a laboratory-scale counter-current centrifugal contactor process. *Solvent Extr. Ion Exch.* **2013**, *31*, 519–537. [CrossRef]
27. Duan, W.; Zhou, X.; Zhang, C. Extraction of Hydrocortisone from the Fermentation Liquor with Annular Centrifugal Contactors. *Sep. Sci. Technol.* **2006**, *41*, 573–581.
28. Bergeonneau, P.; Jaouen, C.; Germain, M.; Bathellier, A. Uranium, neptunium and plutonium kinetics of extraction by tributylphosphate and trilaurylamine in a centrifugal contactor. In Proceedings of the International Solvent Extraction Conference (ISEC-77), Toronto, ON, Canada, 9–16 September 1977; Lucas, B.H., Smith, H.W., Eds.; CEA Centre d'Etudes Nucleaires de Fontenay-aux-Roses: Toronto, ON, Canada, 1977; p. 612.
29. Verlinden, B.; Wilden, A.; Van Hecke, K.; Egberink, R.J.M.; Huskens, J.; Verboom, W.; Hupert, M.; Weßling, P.; Geist, A.; Panak, P.J.; et al. Solvent Optimization Studies for a New EURO-GANEX Process with 2, 2′-Oxybis (N, N-di-n-decylpropanamide)(mTDDGA) and Its Radiolysis Products. *Solvent Extr. Ion Exch.* **2023**, *41*, 59–87. [CrossRef]
30. Leonard, R. *Prediction of Hydraulic Performance in Annular Centrifugal Contactors*; Argonne National Lab: Lemont, IL, USA, 1980.
31. Siczek, A.A.; Meisenhelder, J.H.; Bernstein, G.J.; Steindler, M.J. Solvent extraction studies in miniature centrifugal contactors. *Radiochim. Acta* **1980**, *27*, 51–60. [CrossRef]
32. De Santis, A.; Colombo, M.; Hanson, B.; Fairweather, M. A generalized multiphase modelling approach for multiscale flows. *J. Comput. Phys.* **2021**, *436*, 110321. [CrossRef]
33. De Santis, A.; Hanson, B.; Fairweather, M. Hydrodynamics of Annular Centrifugal Contactors: A CFD analysis using a novel multiphase flow modelling approach. *Chem. Eng. Sci.* **2021**, *242*, 116729. [CrossRef]
34. Colombo, M.; De Santis, A.; Hanson, B.C.; Fairweather, M. A novel generalized multifluid modelling approach for the simulation of multiphase flows: Model development and validation. In Proceedings of the 13th International European Research Community on Flow, Turbulence and Combustion (ERCOFTAC) Symposium, Rhodes, Greece, 15–17 September 2021; Springer: Berlin/Heidelberg, Germany, 2021.
35. De Santis, A.; Colombo, M.; Hanson, B.C.; Fairweather, M. A novel generalized multifluid modelling approach for the simulation of multiphase flows: Application to intensified liquid-liquid extraction. In Proceedings of the 13th International European Research Community on Flow, Turbulence and Combustion (ERCOFTAC) Symposium, Rhodes, Greece, 15–17 September 2021; Springer: Berlin/Heidelberg, Germany, 2021.
36. Fells, A.; De Santis, A.; Colombo, M.; Theobald, D.W.; Fairweather, M.; Muller, F.; Hanson, B. Predicting Mass Transfer in Liquid-Liquid Extraction Columns. *Processes* **2022**, *10*, 968. [CrossRef]
37. De Santis, A.; Colombo, M.; Hanson, B.C.; Fairweather, M. Hydrodynamics and mass transfer in multiscale multiphase flows: A novel CFD modelling approach. In Proceedings of the 19th International Topical Meeting on Nuclear Reactor Thermal Hydraulics (NURETH-19), Brussels, Belgium, 6–11 March 2022; Sheffield American Nuclear Society: Sheffield, UK, 2022.
38. Taylor, R.; Mathers, G. Innovation in the aqueous recycle of spent nuclear fuels. *Nucl. Future* **2019**, *15*, 40–48.
39. Miao, Q.; Sun, T.; Zheng, Q.; Zhang, Y.; Duan, W. Effects of the Structure, Operation, and Physical Parameters on the Actual Phase Ratio and Interface Radius in the Separation Zone of an Annular Centrifugal Contactor. *Ind. Eng. Chem. Res.* **2023**, *62*, 637–648. [CrossRef]
40. Bertelsen, E.R.; Antonio, M.R.; Jensen, M.P.; Shafer, J.C. Electrochemistry of PUREX: R is for reduction and ion transfer. *Solvent Extr. Ion Exch.* **2022**, *40*, 64–85. [CrossRef]